Journal of the Korean Ceramic Society
Vol. 37, 11 pp. 1126-1129 (2000)

Crystallographic Relationships of (Ba, Sr)TiO_3 Thin Film Prepared by Metal-Organic Chemical Vapor Deposition on (111) Textured Pt Electrode

Dong Chul Yoo and Jeong Yong Lee

Department of Materials Science and Engineering,
Korea Advanced Institute of Science and Technology, Taejon, 305-701, Korea
(Received July 8, 2000)

The crystallographic orientations of $Ba_{0.6}Sr_{0.4}TiO_3$ (BST) thin film deposited by a metal-organic chemical vapor deposition on (111) textured Pt electrode were studied with a transmission electron microscopy. The fully crystallized BST thin film (50 nm) has (100) and (110) preferred orientations. A high resolution transmission electron microscopy study has revealed the crystallographic orientation relationships between BST thin film and Pt electrode. These relationships explained the preferred orientation of BST film on (111) textured Pt electrode. With these results, we could represent the atomic arrangement at the BST/Pt interface.

Key words: (Ba,Sr)TiO_3, Transmission electron microscopy (TEM), Crystallographic orientation

I. Introduction

Recently (Ba,Sr)TiO_3 (BST) thin films have received great attentions as dielectric materials for Giga-bit dynamic random access memory (DRAM) capacitor because of their high dielectric character of $BaTiO_3$ and structural endurance of $SrTiO_3$. As the BST is a paraelectric material at room temperature, it has no fatigue effect of ferroelectrics. There are many methods of depositing BST thin film metallo-organic decomposition (MOD),[1] sputtering,[2,3] metal-organic chemical vapor deposition (MOCVD),[4,5] laser ablation,[6] and so on. Among the various deposition methods, MOCVD is a desirable process because of its potential advantages such as the step coverage, high quality, and amenability to large scale processing.

In many difficulties of BST/Pt capacitor, one is the electrical degradation because of an amorphous layer at BST/Pt interface.[7] As a dielectric layer is thinner, an amorphous layer of the interface has worse effect. In addition, the various growth behaviors of dielectric films, such as random, textured, or epitaxial, greatly influence their electrical properties.

In order to understand the growth behavior of BST thin film, it is needed to understand the crystallographic orientation relationships of BST grains on Pt electrode. There have been some reports about interfacial properties and the crystal orientations between BST and different oxide electrodes.[8-10] However, there are few reports regarding crystallographic orientation relationships of BST/Pt interface prepared by MOCVD. In this work, we have studied crystallographic orientations of cubic $Ba_{0.6}Sr_{0.4}TiO_3$ film deposited by MOCVD on (111) textured Pt electrode with a transmission electron microscope (TEM) and showed the desirable atomic arrangement model at BST/Pt interface.

II. Experimental Procedure

$Ba_{0.6}Sr_{0.4}TiO_3$ thin film was prepared by a MOCVD. $Ba(TMHD)_2$, $Sr(TMHD)_2$ and Ti-isopropoxide (TIP) were each used as Ba, Sr and Ti sources. NH_3 gas was used for carrier gas of Ba and Sr sources and Ar gas was used for Ti source.

Ti source was flowed for 30 min and Ba, Sr sources were preheated for 30 min to obtain uniform composition to vertical direction of substrate. A deposited thin film (50 nm) was fast annealed and cooled at RTA at 650°C for 5 min. Pt electrode of about 100 nm was prepared on SiO_2/Si substrate by rf-sputtering.

The orientations of BST film were analyzed by X-ray diffraction (XRD) (Rigaku- D/MAX-IIIC). For TEM observations, cross-sectional specimen was polished about scores of micrometers with mechanical polisher. Then the specimen was ion-milled (GATAN Duomilling) with conditions of 5 kV and 0.6 mA by Ar gas. During ion-milling process, specimen was rotated with sector speed of 60° to minimize the sputtered rate difference between BST and Pt at liquid nitrogen cold trap.

Plane-view specimen was polished about hundreds of micrometers by mechanical polisher and chemically etched. The specimen was ion-milled at low angle (<8°) by Ar gas. Each sample was observed for a high resolution image, a bright field image and a selected area electron diffraction

(SAED) pattern with a TEM (JEOL JEM-2000EX) at 200 kV.

III. Results and Discussion

Fig. 1 shows XRD pattern of BST thin film. Pt has (111) preferred orientation on SiO_2/Si substrate and BST film has a strong intensity at (110) and (200) planes. As the intensity of BST (111) plane is overlapped with that of Pt (111) plane, the BST (111) peak looks like having a strong intensity. However, in fact, the intensity of BST (111) plane is very weak. From a bright field image, the BST film has columnar structure on the Pt electrode. XRD result shows that BST film has the preferred orientation of (110) and (100) planes on (111) textured Pt electrode.

Fig. 2 shows a selected area electron diffraction (SAED) pattern of cross-sectional BST film, where BST (110) and (200) planes are parallel with Pt (111) plane. These are well matched with the XRD result. As no amorphous ring pattern exists in SAED pattern, BST film has been fully crystallized.

Fig. 3 shows SAED pattern of plane-view BST films, where diffracted spots of BST (110) and (200) planes have the same direction and strong intensity. This indicates that the BST (110) and (200) grains have the orientation relationships on (111) textured Pt electrode. In order to find these relationships, we studied the possible crystallographic orientation between BST and Pt.

Fig. 4 shows a schematic representation of crystal planes and atomic distances for BST and Pt. In view of atomic arrangement and distance, the BST (111) plane is very well matched with the Pt (111) plane. However, in spite of good lattice match and atomic arrangement with the Pt (111)

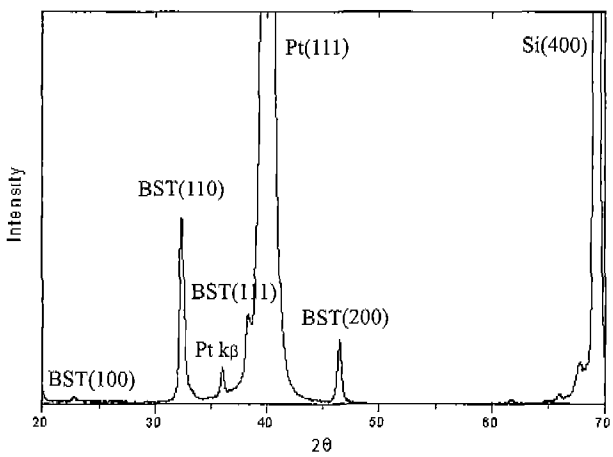

Fig. 1. XRD profile of BST/Pt/SiO_2/Si.

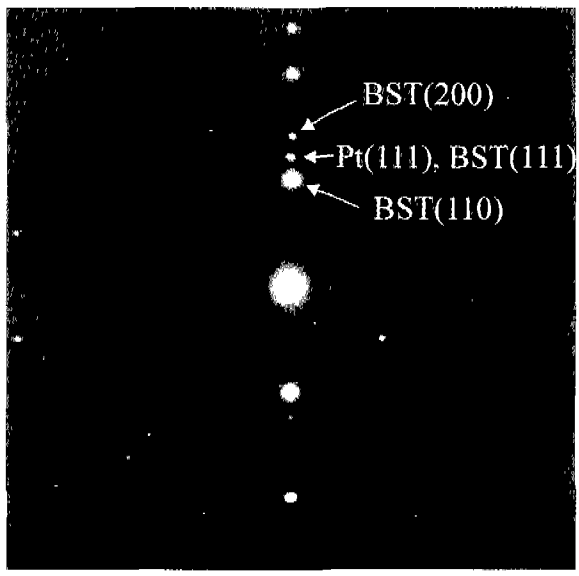

Fig. 2. Cross-sectional selected area electron diffraction pattern of BST/Pt.

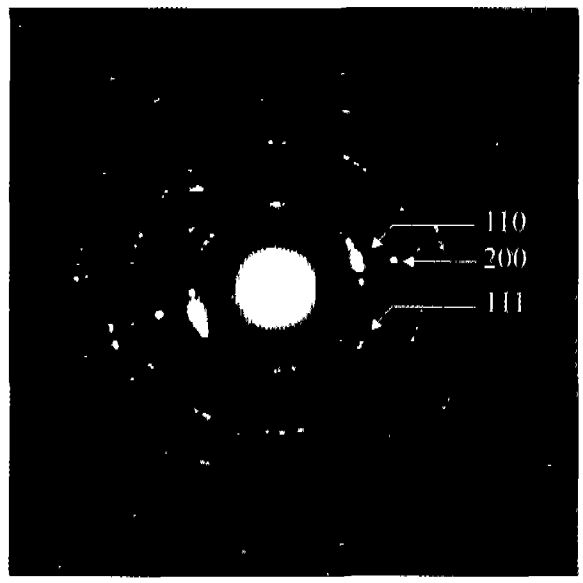

Fig. 3. Plane-view selected area electron diffraction pattern of BST.

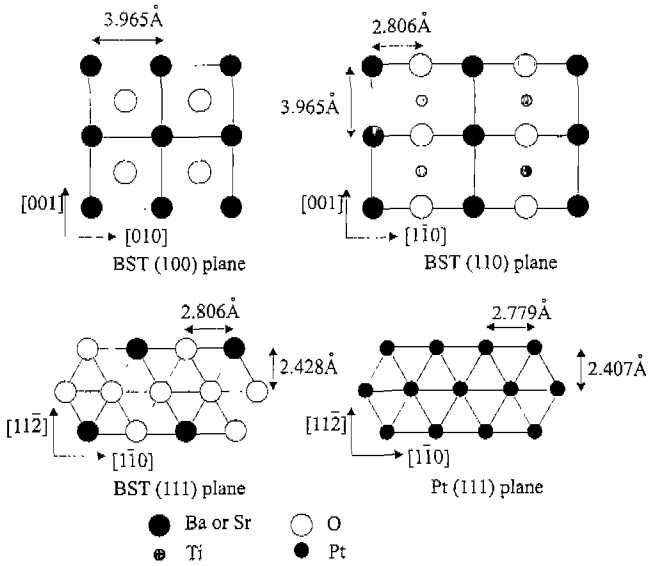

Fig. 4. Atomic distance and direction of BST and Pt planes.

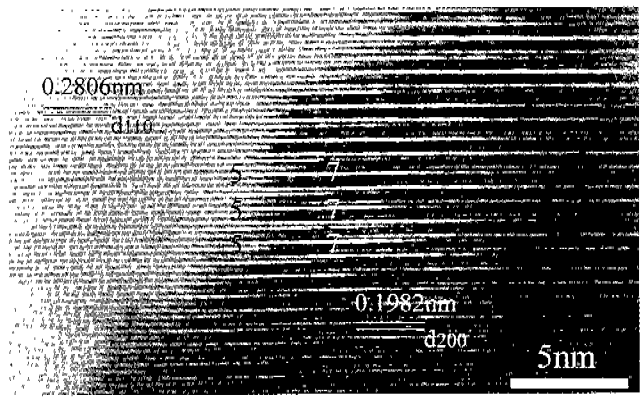

Fig. 5. High resolution TEM micrograph showing the boundary of BST (110) and (100) grains.

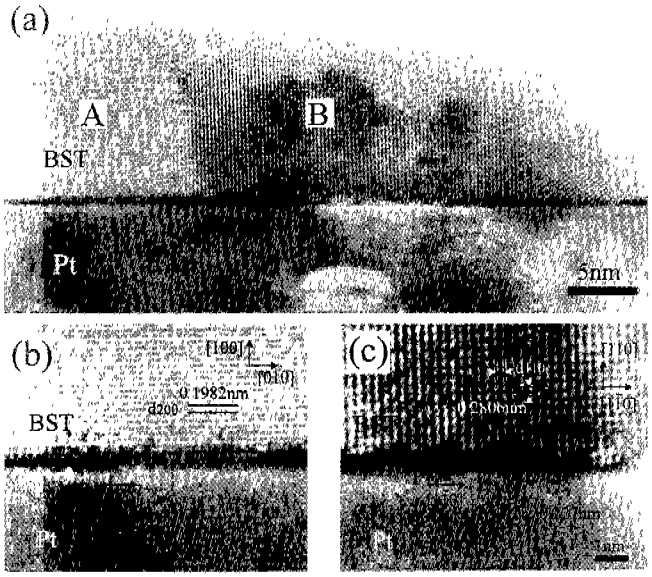

Fig. 6. High resolution TEM micrograph of (a) BST/Pt interface, (b) BST (100) grain in region A and (c) BST (110) grain in region B.

plane, the BST (111) plane must have independent Ti^{+4} ion when the BST film is deposited with (111) plane. However, oxygen atmosphere is a necessity in deposition condition. As Ti^{+4} ion is less stable than Ti-oxide, such as TiO_2 in view of a thermodynamic free energy, this prevents the BST film from being crystallized with (111) plane.[11,12] BST [1$\bar{1}$0] direction in BST (110) plane is well matched with Pt [1$\bar{1}$0] in Pt (111) plane and the lattice mismatch is 0.88%. Therefore, when BST (110) plane is crystallized on Pt (111) plane, BST [1$\bar{1}$0] direction will be parallel with Pt [1$\bar{1}$0] direction. Considered the crystallographic orientation relationships referred above, BST (110) planes are crystallized not with random orientations, but with BST [1$\bar{1}$0] || Pt [1$\bar{1}$0] and BST [001] || Pt [11$\bar{2}$] relationships on (111) textured Pt electrode. Because BST (200) spots as well as BST (110) spots are parallel with Pt (111) plane in SAED pattern, it is needed to investigate orientation relationships between BST (200) plane and Pt (111) plane. In Fig. 4, BST [1$\bar{1}$0] direction of BST (100) plane is well matched with Pt [1$\bar{1}$0] direction in view of lattice matching relation. However, if the [1$\bar{1}$0] direction of (200) planes are parallel with Pt [1$\bar{1}$0] direction on (111) textured Pt electrode, it is impossible for BST $(110)_{(110)\ grain}$ and $(200)_{(100)\ grain}$ spots to have the same direction in the plane-view SAED pattern. Therefore in order to explain this result, a high resolution TEM study was carried out.

Fig. 5 shows a high resolution image of BST film. The left region of image shows BST (110) lattice image and the right region of image shows BST (200) lattice image. This lattice image shows that 5 lines of BST (110) plane are matched with 7 lines of BST (200) plane at the boundary of BST (110) and (100) grains.

Fig. 6(a) is a high resolution image which shows BST (110) grain and BST (100) grain on (111) Pt electrode. In region A, BST (200) planes are parallel with Pt (111) plane and in region B, BST (110) planes are parallel with Pt (111) plane. Fig. 6(b) shows lattice image of BST (100) grain on (111) textured Pt electrode in region A. Fig. 6(c) shows lattice image of BST (110) grain on (111) textured Pt electrode in region B.

From these high resolution images, we can find orientation relationships which are $[010]_{(100)\ grain}$ || $[1\bar{1}0]_{(110)\ grain}$ and $(100)_{(100)\ grain}$ || $(110)_{(110)\ grain}$ at the boundary of BST (110) and BST (100) grains. These relationships are well consistent with SAED patterns.

From the relationships of BST (110) and (100) grains, we can find relationships of BST (100) and Pt (111) plane which are BST [010] || Pt [1$\bar{1}$0] and BST (100) || Pt (111).

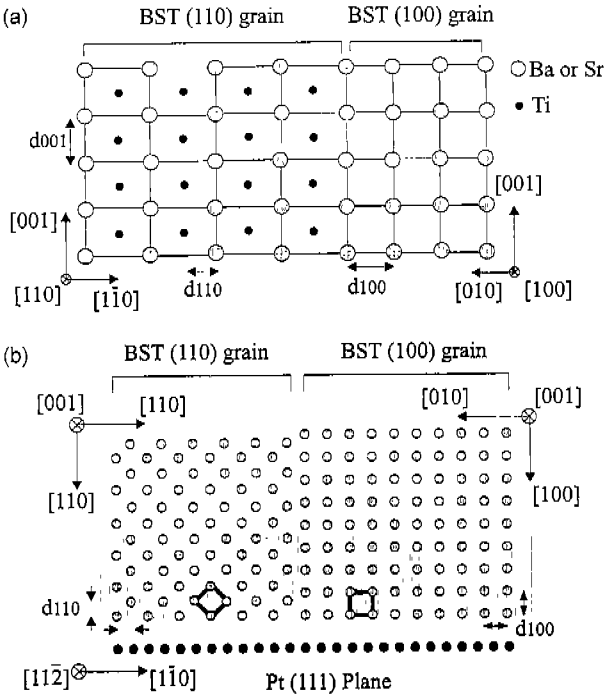

Fig. 7. Schematic representation of atomic arrangements of (a) plane-view BST and (b) cross-sectional BST/Pt interface.

Although [010] direction of BST (100) plane has a relatively large mismatch with [1 $\bar{1}$ 0] direction of Pt (111) plane, BST (100) grains can be grown with the orientation relationship of BST (110) grains on (111) textured Pt electrode. Therefore the orientations of BST (100) grains were more affected by the orientations of BST (110) grains than those of (111) textured Pt electrode.

Fig. 7 shows schematic atomic arrangements of BST (110) and (100) grains on Pt (111) plane. Fig. 7(a) is the representation of plane-view direction. This shows that BST (110) and (100) grains can be grown with sharing the same atoms to the [001] direction. Fig. 7(b) is the cross-sectional representation of BST (110) and (100) grains on (111) textured Pt electrode. In Fig. 7(b), a box region with dotted lines shows that 5 lines of BST (110) plane are matched with 7 lines of BST (200) plane. This is well consistent with the high resolution image in Fig. 5.

Finally, it should be noted that the crystallographic orientation of BST films was strongly related with the orientation of Pt electrode and also related with the orientation between BST grains.

IV. Conclusions

In this work, the crystallographic orientations of BST films on (111) textured Pt electrode were studied with a transmission electron microscope. The BST thin film grown by MOCVD was fully crystallized from BST/ Pt interface without any amorphous layer. BST thin film had the preferred orientation of (110) and (100) planes on (111) textured Pt electrode. At the BST/Pt interface, BST (110) grains had the relations of BST [1 $\bar{1}$ 0] || Pt [1 $\bar{1}$ 0] and BST (110) || Pt (111). At the boundaries of BST (110) and BST (100) grains, the relationships were $[010]_{(100)\ grain}$ || $[1\bar{1}0]_{(110)\ grain}$ and $(100)_{(100)\ grain}$ || $(110)_{(110)\ grain}$. From these relationships, we could find that BST (100) grains had relationships of BST [010] || Pt [1 $\bar{1}$ 0] and BST (100) || Pt (111) on Pt electrode. These relationships between BST and Pt electrode can be expected to be useful to understand the growth behavior of BST film.

Acknowledgments

We acknowledge the support of this research by the Ministry of Science and Technology of Korea through the National Research Laboratory Program.

References

1. S. B. Krupanidhi and C. J. Peng, "Studies on Structural and Electrical Properties of Barium Strontium Titanate Thin Films Developed by Metallo-Organic Decomposition," *Thin Solid Films*, **305**, 144 (1997).
2. C. S. Hwang, B. T. Lee, C. S. Kang, J. W. Kim, K. H. Lee, H. J. Cho, H. Horii, W. D. Kim, S. I. Lee, Y. B. Roh and M. Y. Lee, "A Comparative Study on the Electrical Conduction Mechanism of $(Ba_{0.5}Sr_{0.5})TiO_3$ Thin Films on Pt and IrO_2 Electrodes," *J. Appl. Phys.*, **83**, 3703 (1998).
3. B. A. Baumert, L. H. Chang, A. T. Matsuda, T. L. Tsai, C. J. Tracy, R. B. Gregory, P. L. Fejes, N. G. Cave, W. Chen et. al., "Characterization of Sputtered Barium Strontium Titanate and Strontium Titanate Thin Films," *J. Appl. Phys.*, **82**(5), 2558 (1997).
4. Y. Takeshima, K. Shiratsuyu, H. Takagi and Y. Sakabe, "Preparation and Dielectric Properties of the Multilayer Capacitor with (Ba,Sr)TiO_3 Thin Layers by Metalorganic Chemical Vapor Deposition," *Jpn. J. Appl. Phys.*, **36**, 5870 (1997).
5. G. W. Dietz, M. Schumacher, R. Waser, S. K. Streiffer, C. Basceri and A. I. Kingon, "Leakage Currents in $Ba_{0.7}Sr_{0.3}TiO_3$ Thin Films for Ultrahigh-Density Dynamic Random Access Memories," *J. Appl. Phys.*, **82**(5), 2359 (1997).
6. H. Kobayashi and T. Kobayashi, "Heteroepitaxial Growth of Quaternary $Ba_xSr_{1-x}TiO_3$ Thin Films by ArF Excimer Laser Ablation," *Jpn. J. Appl. Phys.*, **33**, L533 (1994).
7. S. H. Paek, J. H. Won, K. S. Lee, J. S. Choi and C. S. Park, "Electrical and Microstructural Degradation with Decreasing Thickness of (Ba,Sr)TiO_3 Thin Films Deposited by RF Magnetron Sputtering," *Jpn. J. Appl. Phys.*, **35**, 5757 (1996).
8. T. Kawakubo, S. Komatsu, K. Abe, K. Sano, N. Yanase and N. Fukushima, "Ferroelectric Properties of $SrRuO_3$/(Ba,Sr)TiO_3/$SrRuO_3$ Epitaxial Capacitor," *Jpn. J. Appl. Phys.*, **37**, 5108 (1998).
9. D. Y. Noh, H. H. Lee, T. S. Kang and J. H. Je, "Crystallization of Amorphous (Ba,Sr)TiO_3/MgO(001) Thin Films," *Appl. Phys. Lett.*, **72**(22), 2823 (1998).
10. K. Hieda, K. Eguchi, N. Fukushima, T. Aoyama, K. Natori *et. al.*, "All Perovskite Capacitor (APEC) Technology for (Ba,Sr)TiO_3 Capacitor Scaling toward 0.10 μm Stacked DRAMs," *IEDM.*, **30**(2), 807 (1998).
11. C. S. Hwang, M. D. Vaudin and P. K. Schenck, "Influence of the Microstructure of Pt/Si Substrates on Textured Growth of Barium Titanate Thin Films Prepared by Pulsed Laser Deposition," *J. Mater. Res.*, **13**(2), 368 (1998).
12. I. T. Kim, S. J. Chung and S. J. Park, "Microstructure and Preferred Orientation of $BaTiO_3$ Thin Films on Pt/Ti/SiO_2/Substrates Prepared by Ultrasonic Spraying Deposition," *Jpn. J. Appl. Phys.*, **36**, 5840 (1997).